Available online at www.sciencedirect.com

SciVerse ScienceDirect

Ceramics International 38 (2012) 6823–6829

CERAMICS INTERNATIONAL

www.elsevier.com/locate/ceramint

Preparation of SiC nanowires-filled cellular SiCO ceramics from polymeric precursor

Jian-mei Pan[a], Xue-hua Yan[a], Xiao-nong Cheng[a,*], Qing-bo Lu[b], Ming-song Wang[a], Cheng-hua Zhang[a]

[a]Jiangsu University, School of Materials Science and Engineering, No.301, Xuefu Road, Zhenjiang 212013, PR China
[b]School of Energy and Power Engineering, Jiangsu University, Zhenjiang 212013, PR China

Received 13 April 2012; received in revised form 24 May 2012; accepted 25 May 2012
Available online 6 June 2012

Abstract

SiC nanowires-filled cellular SiCO ceramics were prepared using polyurethane sponge as a porous template infiltrated with silicone resin by pyrolysis at 1400 °C under Ar atmosphere. The pyrolysis temperature was an important parameter affecting the formation of SiC nanowires. The as-prepared sample obtained at 1000 °C was composed of SiCO glasses and turbostratic carbon. The SiCO ceramic was further converted into SiO_2 crystals and amorphous carbon by pyrolysis at 1200 °C. With the increasing pyrolysis temperature, SiC nanocrystals embedded in the non-crystalline SiCO matrix were observed. Furthermore, the SiC nanowires were formed in the pores of the SiCO ceramic. The diameters of the SiC nanowires are in the range 80–150 nm and the lengths are up to several tens of micrometers. The growth mechanism of the nanowires was supported by the vapor-solid mechanism.

Keywords: A. Precursors: organic; B. Porosity; D. SiC

1. Introduction

Porous ceramics have received wide attention due to their excellent performances of high-temperature resistance, thermal-shock resistance, high strength and chemical stability for use in a wide range of applications including high-temperature gas purifiers, filters, sensors, tail gas processors, heat-exchangers, electrodes and catalyst carriers [1–6].

The manufactures of inorganic ceramics derived from silicone-containing polymeric precursors have advantages over the traditional methods of ceramic preparation due to the low temperature processing, versatile shaping and designable molecular structure [7,8]. Among the several polymeric precursors available, polysiloxanes were studied extensively due to their lower cost and commercial supply. The polysiloxanes were transformed into amorphous silicon oxycarbide ceramics, described as SiC_xO_{4-x} ($0 \le x \le 4$), or simply SiC_xO_y or SiCO, in an inert atmosphere above 1000 °C [9–11]. In the previous work, the replica technique was widely used for preparing porous SiCO or SiC ceramics from polymeric precursors [12–14]. For example, SiCO/C-ceramic composites were prepared from chemically modified wood templates infiltrated with polymethylhydrosiloxane (PMHS) [15]. Polyurethane (PU) sponge was coated with or immersed in a polymeric suspension or precursor solution to produce porous ceramics [16–18]. Edirisinghe et al. [19–21] developed a simple method to produce porous SiC ceramics by immersing the PU foam in a polysilane precursor solution. Vogt et al. [22] prepared macroporous nitrogen-based silicone carbide (NBSiC) ceramics by immersing the PU sponge in a polysiloxane (MK polymer) precursor slurry. It is well known that SiC nanowires have the great properties such as high temperature strength, chemical stability, thermal shock resistance and field emission properties [23–26]. Therefore, SiC nanowires have a great potential to be used as reinforcing element in ceramic, metal and polymer–matrix composites. There are several routes to synthesize SiC nanowires, such as chemical vapor deposition, through reaction of silica and

*Corresponding author. Tel.: +86 0511 88780006; fax: +86 0511 88791739.
E-mail address: xncheng@ujs.edu.cn (X.-n. Cheng).

0272-8842/$36.00
http://dx.doi.org/10.1016/j.ceramint.2012.05.081

carbon solid mixtures, by reduction of methyl trichlorosilane, by reaction of Si_3N_4 with carbon, and by thermal decomposition of rice husk [27–30]. It can be concluded that the porous bodies can provide enough growth space for nanowires [31,32]. However, little work has been reported on SiC nanowires-filled porous ceramics using PU sponge as a porous template in the literature.

In the present work, we attempted to fabricate SiC nanowires-filled cellular SiCO ceramics without a metal catalyst, using PU sponge as a template infiltrated with silicone resin. The silicone resin was used as a source for the growth of the SiC nanowires. The as-prepared samples were characterized by TG, XRD, FTIR, SEM, and TEM. The growth mechanism of the SiC nanowires has been tentatively suggested.

2. Experimental procedure

Commercially available PU sponge with a size of 30 mm × 30 mm × 5 mm was used as a template. Commercially available silicone resin (solid content: 48–52%, Tu-4 cup viscosity at 25 °C: 18–35 s, Changzhou Jianuo Organosilicone Co., Ltd., Jiangsu, China) was used as a polymeric precursor. The mass ratio of the silicone resin and the PU sponge was 20:1. The silicone resin was adequately absorbed in the sponge, and then was dried at 125 °C for 8 h under vacuum drying oven. The above process was repeated three times. The pyrolysis of the samples was carried out in a tube furnace under a constant flow of argon gas at a rate of 0.2 L/min. The green bodies were heated at a rate of 5 °C/min up to 150 °C for 15 min and a lower rate of 2 °C/min up to 400° C for 30 min, then at a rate of 5 °C/min up to the desired temperatures (1000 °C, 1200 °C and 1400 °C) for 3 h. The specimens were cooled down to 400 °C with a rate of 3 °C/min then down to room temperature.

The thermogravimetric measurement was investigated using thermogravimetry-differential scanning calorimetry (TG-DSC, STA449C, Germany) in Ar with a heating rate of 10 °C/min. The phase identification was measured by X-ray diffractometer (XRD, D/max 2550 V, Japan) using a nickel filtered CuKα radiation produced at 35 kV and 20 mA. The infrared absorption spectra were obtained using Fourier transform infrared spectrometer (FTIR, Nicolet-460, America) in the range 3200–500 cm^{-1}. The morphological structures of the samples were observed using scanning electron microscope (SEM, JSM-7001 F, Japan). The elemental composition of the samples was analyzed by energy-dispersive X-ray spectroscopy (EDS) attached to SEM. The microstructure of the samples was further characterized by a field emission transmission electron microscope (TEM, H-800, Japan) and high resolution TEM (HRTEM, JEM-2100, Japan). The specific surface area measurements of the samples were carried out by degassing at 400 °C for 2 h, followed by N_2 adsorption at 77 K, using an automatic apparatus (NOVA2000, USA), and the specific surface areas were calculated from the isotherms by the Brunauer–Emmett–Teller (BET) method. The volume resistivities of the samples were measured by the four-probe method (RTS-9, China).

3. Results and discussion

3.1. Decomposition behavior of the PU sponge and polymeric precursor

The decomposition behavior of the silicone resin and the PU sponge in argon atmosphere was examined by TG-DSC, as shown in Fig. 1. It is noteworthy that the thermal decomposition of the PU sponge starts at about 230 °C and nearly 85 wt% of the material is lost by 400 °C. It can be found that the PU sponge is almost fully pyrolyzed at 510 °C. The silicone resin presents an initial weight loss of about 40 wt% probably due to the volatilization of the physically adsorbed water and the curing of the silicone resin at a lower temperature. DSC curve shows an endothermic peak at 92 °C. The second weight loss of about 11 wt% of the silicone resin (from 160 °C up to 520 °C) presents a gentle sloping baseline. This weight loss is due to the degradation reactions of the Si–O polymer chain and redistribution reactions of different silicon sites. The third weight loss of approximately 8 wt% is related to the polymer-to-ceramic conversion corresponding to an exothermic peak which appeared at 805 °C in the DSC curve.

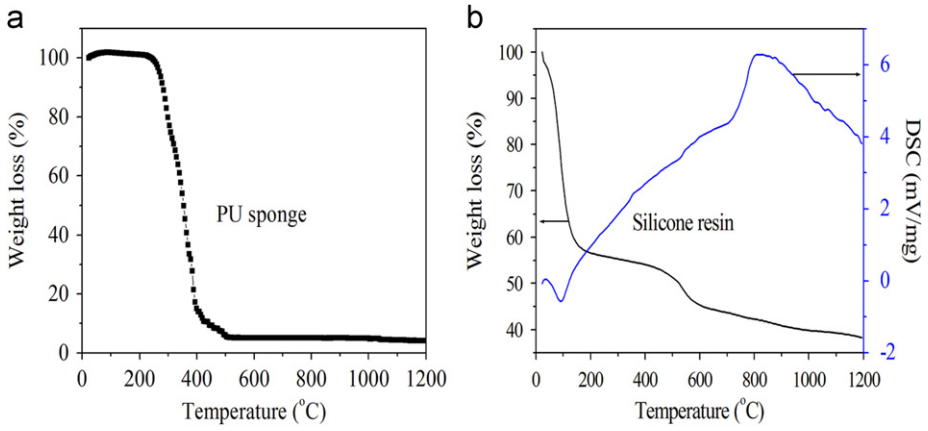

Fig. 1. TG–DSC curves of the PU sponge and silicone resin in Ar atmosphere.

3.2. Sample characterization

Fig. 2 shows the XRD patterns of the as-prepared samples obtained at different temperatures. X-ray pattern of the sample obtained at 1000 °C displays the characteristic of an amorphous material. The broad diffraction peak at $2\theta \approx 22^\circ$ of the samples corresponds to the amorphous SiOC glasses [33]. Furthermore, the turbostratic graphite-like phase was found to be present in the sample, with a discernible broad diffraction reflex at $2\theta \approx 43^\circ$. With a further increase in temperature, the diffraction peaks at 2θ of 20.8° and 26.6° appear, indicating that the SiO_2 crystals were formed (JCPDS Card no. 65-0466). XRD pattern of the sample obtained at 1400 °C shows the crystalline peaks at 2θ of 35.6°, 60.0° and 71.8° corresponding to the diffraction from the (111), (220) and (311) lattice planes of β-SiC, respectively (JCPDS Card no. 29-1129).

Fig. 3 shows the FTIR spectra of the samples prepared at different temperatures. The spectrum of the sample treated at 1000 °C indicates that the typical vibration bands at 2930–2850 cm^{-1} are assigned to the C–H absorptions. In addition, the bands located at 1680–1620 cm^{-1} are due to the vibration of the C═C bonds. The weak bands at 1120–1030 cm^{-1} are assigned to the typical Si–O absorptions. The spectrum of the sample obtained at 1200 °C shows a strong absorption band at 1063 cm^{-1}, which is assigned to the Si–O bonds. The band from 690 cm^{-1} to 890 cm^{-1}, characteristic of Si–C sites, could be observed. The spectrum of the sample prepared at 1400 °C shows a band centered at 843 cm^{-1} due to the Si–C vibration. The absorption peak of the Si–C bonds displays a higher intensity at 1400 °C, and Si–O bonds disappear gradually with the increasing temperature, indicating that the Si–O bonds were transformed into Si–C bonds during the pyrolysis process.

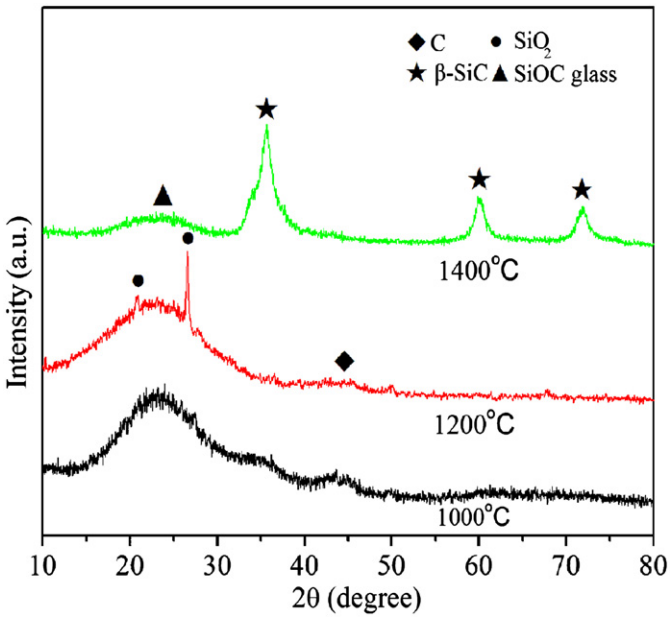

Fig. 2. XRD patterns of the as-prepared samples obtained at different temperatures.

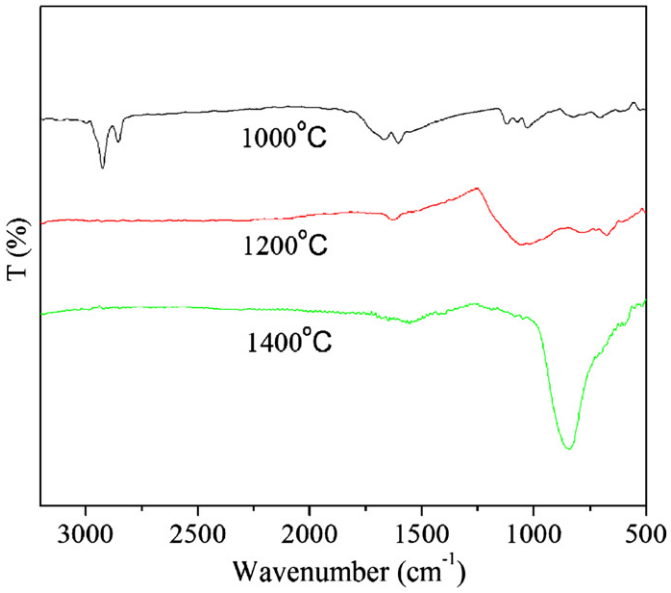

Fig. 3. FTIR spectra of the as-prepared samples obtained at different temperatures.

Fig. 4a shows the SEM image of the PU sponge with pore sizes in the range 200 − 500 μm. The sample obtained at 1200 °C reserves the cellular feature of the PU sponge, as shown in Fig. 4b.Fig. 4c shows the high-magnification SEM image. The SEM image displays two distinct regions. The first one is the black region, The EDS analysis indicates that the surface is composed of Si, O and C, which is in agreement with SiCO ceramic. The second one shows the particles with different morphologies dispersed on the surface of the SiCO ceramic. The EDS analysis indicates that the particle contains Si and O. The O/Si atomic ratio within the particles is higher than that in the bulk SiOC ceramic. Usually, the increase of the pyrolysis temperature above 1200 °C results in a phase separation of the SiCO amorphous network into SiO_2 and nanocrystalline β-SiC [9,34]. It can be assumed that the particles are SiO_2 crystals derived from redistribution reactions of different silicon sites. These results agree well with the above XRD analysis.

Fig. 5 shows the SEM images of the as-prepared sample obtained at 1400 °C. The net-like structural feature of the sponge is not changed with the increasing temperature, as shown in Fig. 5a. The EDS analysis corresponding to the selected area in Fig. 5a indicates that the surface of the sample is composed of Si, O and C, as shown in Fig. 5b. However, the irregularly shaped particles were not observed on the surface of the SiCO ceramic. It is a reasonable assumption that the particles can react with residual carbon or CO. Zhong et al. reported different reaction pathways of carbothermic reduction from silica [35]. It is well accepted that SiC formation from carbothermic reduction occurs through the following overall reaction (1). When SiO_2 is in direct contact with C, reaction (2) occurs. When SiO_2 is not in contact with C, reaction (3) is written as follows.

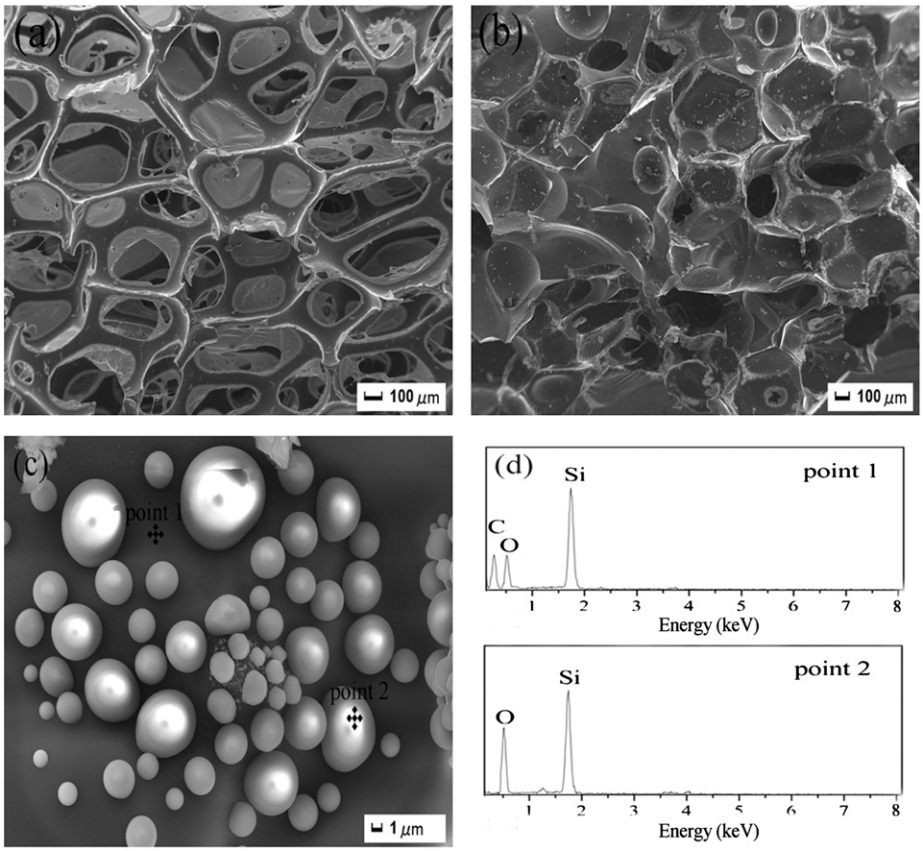

Fig. 4. SEM image of the PU sponge (a), SEM image of the fracture surface of ceramic product obtained at 1200 °C (b), SEM image of the particles on the surface of the ceramic product (c), and EDS spectra corresponding to the selected areas (d).

Furthermore, an alternative reaction pathway in the absence of direct SiO_2 and C contact has also been proposed. The SiO_2 is dissociated according to reaction (4).

$$SiO_{2(s)} + 3C_{(s)} \rightarrow SiC_{(s)} + 2CO_{(g)} \quad (1)$$

$$SiO_{2(s)} + C_{(s)} \rightarrow SiO_{(g)} + CO_{(g)} \quad (2)$$

$$SiO_{2(s)} + CO_{(s)} \rightarrow SiO_{(g)} + CO_{2(g)} \quad (3)$$

$$SiO_{2(s)} \rightarrow SiO_{(g)} + \frac{1}{2}O_{2(g)} \quad (4)$$

However, a white felt layer was produced in the pores of the SiCO ceramic matrix, as can be seen in Fig. 5c. Fig. 5d shows that the white felt layer was a high amount of nanowires. It can be found that the lengths of these nanowires are up to several tens of micrometers. The high-magnification image confirms that the nanowires display different features with curved or straight structures, as shown in Fig. 5e. Fig. 5f shows the SEM image of a single nanowire with an interesting chain-like structure. The diameters of the nanowire are in the range 80–150 nm. The EDS analysis in Fig. 5g indicates that the nanowire contains Si and C. According to the above analysis, it is proposed that the products are SiC nanowires.

Further characterization of the synthesized nanowires was carried out using TEM and HRTEM. Fig. 6a displays a typical TEM image of the nanowire with chain-like structure. The diameter of the nanowire is about 85 nm and the length is up to 8 μm. The corresponding selected-area electron diffraction (SAED) pattern indicates that the nanowire is a single crystal of cubic SiC. As shown in Fig. 6b, a representative HRTEM image indicates that the interplanar spacing is about 0.25 nm, corresponding to the separation between the (111) adjacent lattice planes of β-SiC. It can be concluded that the growth of these SiC nanowire is along the [111] direction. HRTEM image of the SiCO ceramic pyrolyzed at 1400 °C can be seen in Fig. 6c. The crystalline planes with d-spacing of 0.25 nm corresponding to the (111) planes of β-SiC and turbostratic graphite-like phase, with spacing of 0.35 nm assigned to their (002) planes, embedded in a non-crystalline SiCO matrix, were observed. The orientation of the graphite basal planes is indicated by white guidelines.

3.3. Formation mechanism of SiC nanowires

A scheme of processing strategies for the preparation of SiC nanowires-filled cellular SiCO ceramics is shown in Fig. 7. The formation and evolution process can be divided into three stages as follows: (1) the template impregnated with silicone resin solution, (2) curing of the template, and (3) pyrolysis at 1400 °C. In the first stage, the PU sponge was absorbed in the silicone resin. The silicone resin was used to reinforce the wall of the pores, and also used as a

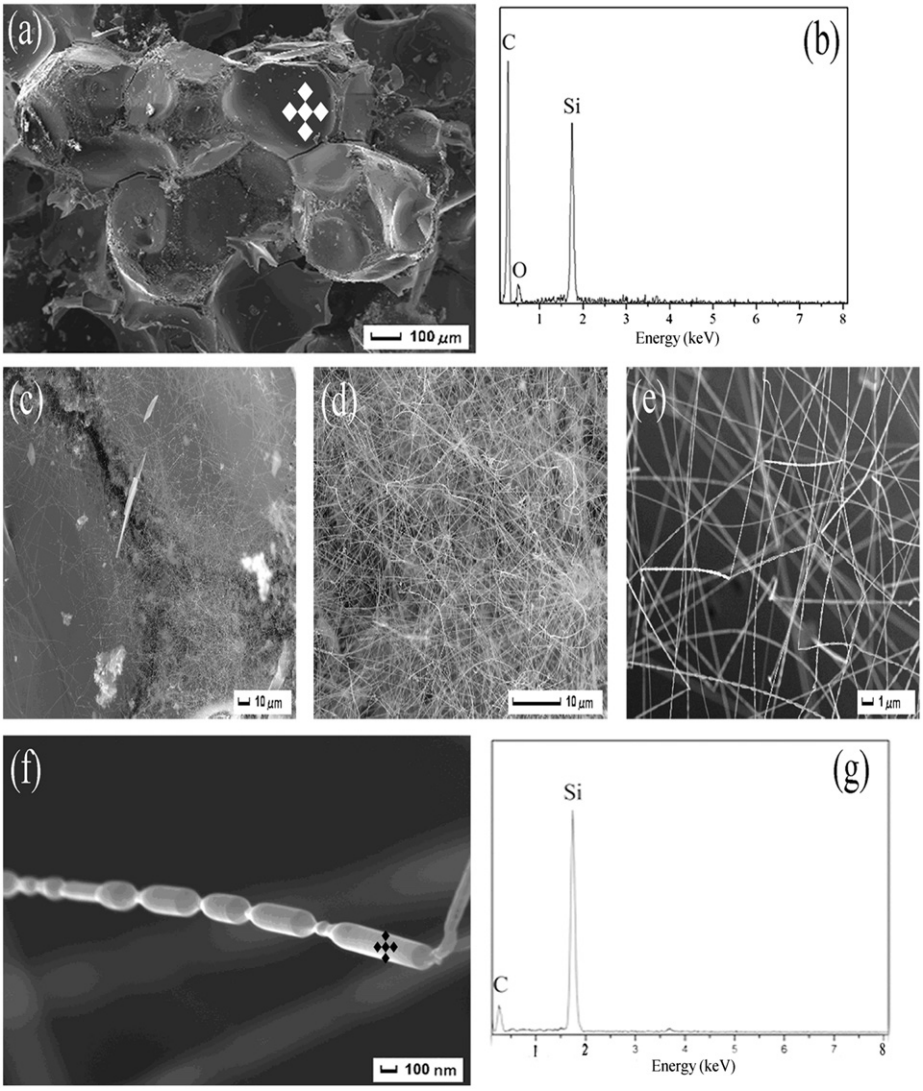

Fig. 5. SEM image of the fracture surface of the as-prepared sample obtained at 1400 °C (a), (b) EDS spectrum corresponding to the selected area in (a), SEM images of the nanowires at various magnifications (c–f), (g) EDS spectrum corresponding to the selected area in (e).

source for the growth of SiC nanowires. As a result, it is predicted that the silicone resin plays a key role on the growth of SiC nanowires. In the second stage, the template was cured via the silanol condensation. Finally, the green bodies were sintered at a high temperature to synthesize SiC nanowires.

The main explanations for the growth of the SiC nanowires are the vapor–liquid–solid (VLS) and vapor–solid (VS) mechanisms [36]. In this study, no droplets were found on the tips of the nanowires. On the basis of the above discussion, a more important contribution for the formation of the nanowires can be attributed to reactions (5) and (6):

$$SiO_{(g)} + 3CO_{(g)} \rightarrow SiC_{(s)} + 2CO_{2(g)} \quad (5)$$

$$C_{(s)} + CO_{2(g)} \rightarrow 2CO_{(g)} \quad (6)$$

The overall reaction (7) can be written as follows:

$$SiO_{(g)} + C_{(s)} \rightarrow SiC_{(s)} + CO_{(g)} \quad (7)$$

The whole reaction was related to the SiO vapor and carbon without a metal catalyst. The diffusion in the vapor–solid phase or the vapor–vapor phase is sufficiently faster than that of the solid–solid (SiO_2 and C) phase. Furthermore, the cellular template has enough flow space for the mass transport of the gaseous species (SiO and CO). Therefore, it can be concluded that the VS mechanism is supposed to govern the growth of the nanowires.

In order to evaluate the possible applications of the samples, the open porosities, specific surface areas and volume resistivities of the as-prepared samples were measured and summarized in Table 1. The highest porosity of the sample obtained at 1400 °C was related to a higher pyrolysis degree and the reaction of carbon with SiO gases. The specific surface area was remarkably increased from 0.5 m^2/g to 45 m^2/g due to the formation of SiC nanowires. It can be found that the volume resistivity of the as-prepared samples had a great change with the increasing temperature. The sample obtained at 1400 °C presents the

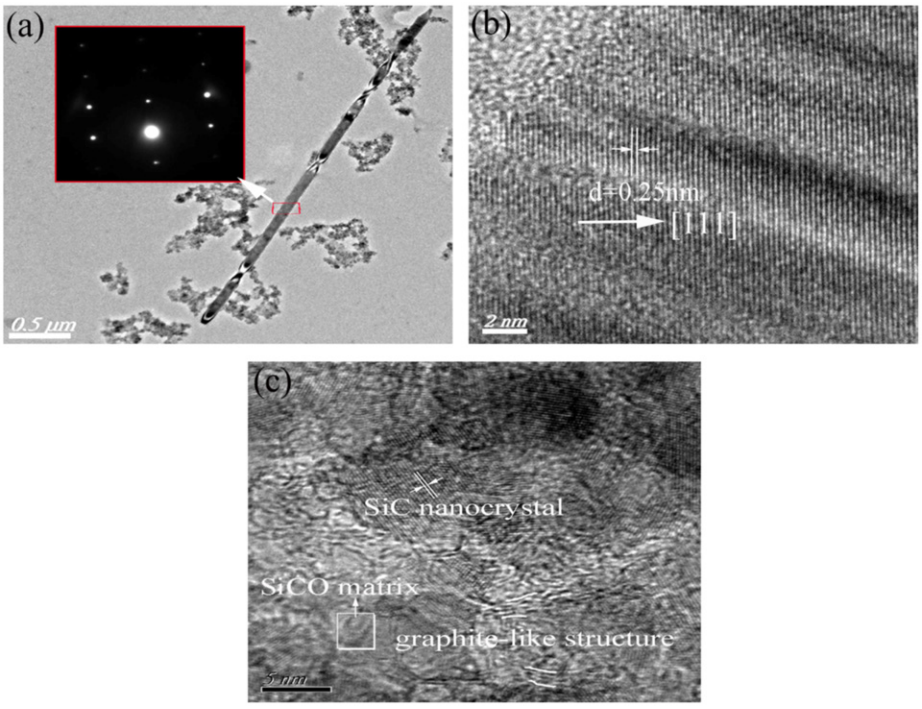

Fig. 6. TEM image of the nanowire and the corresponding SAED pattern (a), HRTEM image of the nanowire (b), and HRTEM image from the ceramic product obtained at 1400 °C (c).

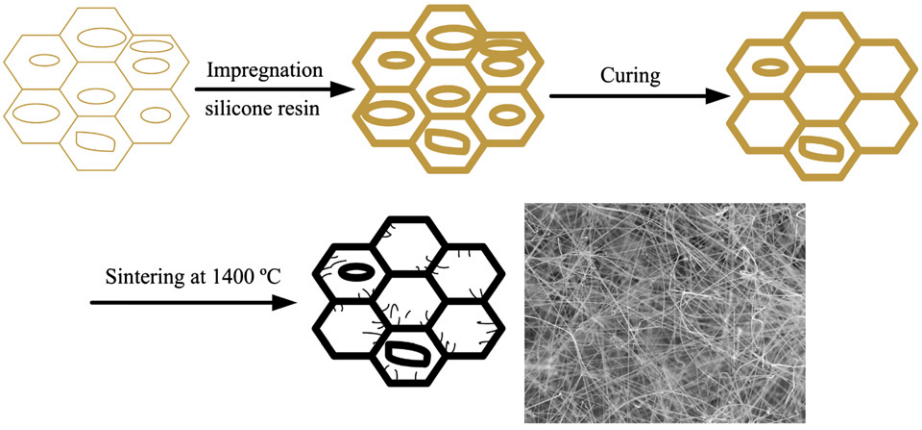

Fig. 7. Schematic illustration for preparing SiC nanowires-filled cellular SiCO ceramics.

Table 1
Porosities, specific surface areas and volume resistivities of the samples at different temperatures.

Temperature (°C)	Porosity (%)	Specific surface area (m^2/g)	Volume resistivity (Ω cm)
1000	76.8	0.5	0.785
1200	81.5	0.8	0.432
1400	85.4	45	0.065

lowest volume resistivity due to the conversion of amorphous SiCO ceramic into crystalline SiC ceramic and the formation of the SiC nanowires.

4. Conclusions

SiC nanowires-filled cellular SiCO ceramics were prepared at 1400 °C using PU sponge as a porous template through a precursor infiltration and pyrolysis route. The sample obtained at 1000 °C was amorphous. SiO_2 particles with different morphologies were observed on the surface of the SiCO ceramic at 1200 °C. With a further increase in temperature, the Si–O bonds of the samples gradually transformed into Si–C bonds during the pyrolysis process. SiC nanowires with curved or straight or chain structures were observed in the pores of the SiCO ceramic. SiC nanowires are up to several tens of micrometers in length and the diameters are in the range 80–150 nm. The VS

mechanism is used to explain the growth process of the nanowires. The presence of SiC nanowires in the porous ceramics caused the increase considerably in the specific surface area and decrease in the volume resistivity.

Acknowledgments

This work was supported by the Materials Tribology Key Laboratory of Jiangsu Opening Foundation (kjsmcx07005), the Natural Science Foundation of the Jiangsu High Education (08KJD430010), the Postgraduate Research and Innovation Project of Ordinary University in Jiangsu Province (CXZZ11_0558), the Talent Foundation of Jiangsu University (09jdg033), the Changshu Research Project (CG201005) and the Excellent Young Teacher of Jiangsu for financial support.

References

[1] C. Vakifahmetoglu, I. Menapace, A. Hirsch, L. Biasetto, R. Hauser, R. Riedel, P. Colombo, Highly porous macro- and micro-cellular ceramics from a polysilazane precursor, Ceramics International 35 (2009) 3281–3290.
[2] D.L. Sun, X.H. Yu, W.J. Liu, D.B. Sun, Laminated biomorphous SiC/Si porous ceramics made from wood veneer, Materials Design 34 (2012) 528–532.
[3] P. Colombo, Engineering porosity in polymer-derived ceramics, Journal of the European Ceramic Society 28 (2008) 1389–1395.
[4] R. Zhuo, P. Colombo, C. Pantano, E.A. Vogler, Silicon oxycarbide glasses for blood-contact applications, Acta Biomaterialia 1 (2005) 583–589.
[5] L. Biasetto, A. Francis, P. Palade, G. Principi, P. Colombo, Polymerderived microcellular SiOC foams with magnetic functionality, Journal of Materials Science 43 (2008) 4119–4126.
[6] P. Colombo, T. Gambaryan-Roisman, M. Scheffler, P. Buhler, P. Greil, Conductive ceramic foams from preceramic polymers, Journal of the American Ceramic Society 84 (2001) 2265–2268.
[7] R. Riedel, M. Seher, J. Mayerd, D.Vinga Szabó, Polymer-derived Si-based bulk ceramics, Part I: preparation, processing and properties, Journal of the European Ceramic Society 15 (1995) 703–715.
[8] J. Mayer, D. Vinga Szabó, M. Rühle, M. Seher, R. Riedel, Polymer-derived Si-based bulk ceramics, Part II: microstructural characterisation by electron spectroscopic imaging, Journal of the European Ceramic Society 15 (1995) 717–727.
[9] A. Saha, R. Raj, Crystallization maps for SiCO amorphous ceramics, Journal of the American Ceramic Society 90 (2007) 578–583.
[10] J.H. Eom, Y.W. Kim, Processing and properties of polysiloxane-derived porous silicone carbide ceramics using hollow microspheres as templates, Journal of the European Ceramic Society 28 (2008) 1029–1035.
[11] Q. Wei, E. Pippel, J. Woltersdorf, M. Scheffler, P. Greil, Interfacial SiC formation in polysiloxane-derived Si–O–C ceramics, Materials Chemistry and Physics 73 (2002) 281–289.
[12] B.V. Manoj Kumar, Y.W. Kim, Processing of polysiloxane-derived porous ceramics: a review, Science and Technology of Advanced Materials 11 (2010) 044303–044318.
[13] P. Colombo, E. Bernardoc, Macro- and micro-cellular porous ceramics from preceramic polymers, Composites Science and Technology 63 (2003) 2353–2359.
[14] R. Rocha, E. Moura, A. Bressiani, J. Bressiani, SiOC ceramic foams synthesized from electron beam irradiated methylsilicone resin, Journal of Materials Science 43 (2008) 4466–4474.
[15] C. Zollfrank, R. Kladny, H. Sieber, P. Greil, Biomorphous SiOC/C-ceramic composites from chemically modified wood templates, Journal of the European Ceramic Society 24 (2004) 479–487.
[16] P. Colombo, J.R. Hellmann, D.L. Shelleman, Mechanical properties of silicon oxycarbide ceramic foams, Journal of the American Ceramic Society 84 (2001) 2245–2251.
[17] P. Colombo, M. Modesti, Silicon oxycarbide ceramic foams from a preceramic polymer, Journal of the American Ceramic Society 82 (1999) 573–578.
[18] P. Colombo, E. Bernardo, L. Biasetto, Novel microcellular ceramics from a silicone resin, Journal of the American Ceramic Society 87 (2004) 152–154.
[19] X. Bao, M.R. Nangrejo, M.J. Edirisinghe, Preparation of silicone carbide foams using polymeric precursor solutions, Journal of Materials Science 35 (2000) 4365–4372.
[20] M.R. Nangrejo, M.J. Edirisinghe, Porosity and strength of silicon carbide foams prepared using preceramic polymers, Journal of Porous Materials 9 (2002) 131–140.
[21] M.R. Nangrejo, X. Bao, M.J. Edirisinghe, Preparation of silicon carbide-silicon nitride composite foams from pre-ceramic polymers, Journal of the European Ceramic Society 20 (2000) 1777–1785.
[22] U.F. Vogt, L. Györfy, A. Herzog, T. Graule, G. Plesch, Macro-porous silicon carbide foams for porous burner applications and catalyst supports, Journal of Physics and Chemistry of Solids 68 (2007) 1234–1238.
[23] E.W. Wong, P.E. Sheehan, C.M. Lieber, Nanobeam mechanics: elasticity, strength and toughness of nanorods and nanotubes, Science 277 (1997) 1971–1975.
[24] K.W. Wong, X.T. Zhou, F.C.K. Au, H.L. Lai, C.S. Lee, S.T. Lee, Field emission characteristics of SiC nanowires prepared by chemical vapour deposition, Applied Physics Letters 75 (1999) 2918–2920.
[25] H.W. Shim, J.D. Kuppers, H. Huang, High-temperature stability of silicon carbide nanowires, Journal of Nanoscience and Nanotechnology 8 (2008) 3999–4002.
[26] C.A. Wang, H. Yong, H.X. Zhai, The effect of whisker orientation in SiC whisker-reinforced Si_3N_4 ceramic matrix composites, Journal of the European Ceramic Society 19 (1999) 1903–1909.
[27] S. Cetinkaya, S. Eroglu, Chemical vapor deposition of C on SiO_2 and subsequent carbothermal reduction for the synthesis of nanocrystalline SiC particles/nanowires, International Journal of Refractory Metals and Hard Materials 29 (2011) 566–572.
[28] V. Krishnarao, Y.R. Mahajan, Formation of SiC nanowires from raw rice husks in argon atmosphere, Ceramics International 22 (1999) 353–358.
[29] P.C. Silva, J.L. Figueiredo, Production of SiC and Si_3N_4 nanowires in C + SiO_2 solid mixtures, Materials Chemistry and Physics 72 (2001) 326–331.
[30] Q.G. Fu, H.J. Li, X.H. Shi, K.Z. Li, Z.B. Hu, J. Wei, Microstructure and growth mechanism of SiC nanowires on carbon/carbon composites prepared by CVD, Materials Letters 59 (2005) 2593–2597.
[31] H.J. Hu, W.C. Zhou, F. Luo, D.M. Zhu, J. Xu, A new synthesis method for producing Si_3N_4 nanowires by heat treating porous Si objects, Journal of the American Ceramic Society 91 (2008) 3800–3802.
[32] B.H. Yoon, C.S. Park, H.E. Kim, Y.H. Koh, In situ synthesis of porous silicone carbide (SiC) ceramics decorated with SiC nanowires, Journal of the American Ceramic Society 9 (2007) 3759–3766.
[33] M. Segatelli, A. Pires, I. Yoshida, Synthesis and structural characterization of carbon-rich SiC_xO_y derived from a Ni-containing hybrid polymer, Journal of the European Ceramic Society 28 (2008) 2247–2257.
[34] H.J. Kleebe, C. Turquat, G.D. Sorarù, Phase separation in an SiCO glass studied by transmission electron microscopy and electron energy-loss spectroscopy, Journal of the American Ceramic Society 84 (2001) 1073–1080.
[35] Y. Zhong, L.L. Shaw, M. Manjarres, M.F. Zawrah, Synthesis of silicon carbide nanopowder using silica fume, Journal of the American Ceramic Society 93 (2010) 3159–3167.
[36] M. Saito, S. Nagashima, A. Kato, Crystal growth of SiC whisker from the SiO(g)–CO System, Journal of Materials Science Letters 11 (1992) 373–376.